

UNCLASSIFIED

RM No. L7101  
Copy No.

~~CONFIDENTIAL~~

7

6412

# NACA

## RESEARCH MEMORANDUM

15 FEB 1947

COMPARISON OF THE TRANSONIC DRAG CHARACTERISTICS  
OF TWO WING-BODY COMBINATIONS DIFFERING ONLY  
IN THE LOCATION OF THE 45° SWEEPBACK WING

By Charles W. Mathews and Jim Rogers Thompson

Langley Memorial Aeronautical Laboratory  
Langley Field, Va.

CLASSIFICATION CANCELLED

CLASSIFIED DOCUMENT Authority Rule 27.23.54 Date 8/18/54

This document contains classified information affecting the National Defense of the United States within the meaning of the Espionage Act, USC 50(a) and (c). Its transmission or the revelation of its contents in any manner to an unauthorized person is prohibited by law. Information so classified may be imparted only to persons in the military and naval services of the United States, approved civilian officers and employees of the Federal Government who have a legitimate interest therein, and to United States citizens of known loyalty and discretion who of necessity must be entrusted therewith.

9/1/54 See

### NATIONAL ADVISORY COMMITTEE FOR AERONAUTICS

WASHINGTON

December 8, 1947

UNCLASSIFIED

NACA LIBRARY

LANGLEY MEMORIAL AERONAUTICAL  
LABORATORY  
Langley Field, Va.

~~CONFIDENTIAL~~

## NATIONAL ADVISORY COMMITTEE FOR AERONAUTICS

## RESEARCH MEMORANDUM

3 1176 01360 8337

COMPARISON OF THE TRANSONIC DRAG CHARACTERISTICS  
OF TWO WING-BODY COMBINATIONS DIFFERING ONLY  
IN THE LOCATION OF THE 45° SWEEPBACK WING

By Charles W. Mathews and Jim Rogers Thompson

## SUMMARY

The Flight Research Division of the NACA Langley Laboratory is measuring the drag of a series of wing-body combinations by the free-fall method in order to provide information on the drag characteristics of promising transonic and supersonic airplane arrangements. This series has so far been limited to a family of swept wings combined with identical body-tail arrangements. Results are presented herein for a configuration having a body of revolution of fineness ratio 12 and a 45° sweptback wing mounted aft of the maximum diameter of the body. These results show that the drag per unit frontal area of this configuration rose from 0.045 of atmospheric pressure at a Mach number of 0.93 to 0.126 of atmospheric pressure at a Mach number of 1.03 and then increased almost linearly to 0.233 at a Mach number of 1.24.

Comparison of these results with those for a previously tested configuration differing only in the location of the wing shows that changing the wing location from a position forward of the body maximum diameter to a position aft of the body maximum diameter decreased the over-all drag by about 35 percent near a Mach number of 1.00 and by about 10 percent at a Mach number of 1.18. The major part of these drag differences was due to differences in the body drag. Comparison of the body drag results for the winged configurations with the results obtained for the body-tail arrangement tested without wings shows that a large favorable interference effect on the body drag occurred with the wing in the aft position and a smaller unfavorable interference effect on the body drag occurred with the wing in the forward position. Thus, a swept wing may be located on a body of this type in such a way as to either increase or decrease the body drag. For both winged configurations the wing drag showed an abrupt rise near a Mach number of 1.00 which did not occur for previous tests of sweptback airfoils mounted on cylindrical bodies. This drag rise, however, is small in comparison to the drag rise associated with rectangular plan-form airfoils.

## INTRODUCTION

Free-fall tests of a series of wing-body combinations are being conducted by the Flight Research Division of the NACA Langley Laboratory. The object of these tests is to determine the drag characteristics of promising transonic and supersonic airplane components. The series has so far been limited to a family of swept wings combined with identical body-tail arrangements. The drag characteristics of the body-tail arrangement tested without wings are reported in reference 1.

The results of a test of one configuration of this series, which consisted of a  $45^\circ$  sweptback wing mounted forward of the maximum diameter of the body, are reported in reference 2. Comparison of these results with those for the body-tail arrangement alone and for  $45^\circ$  sweptback airfoils mounted on cylindrical bodies indicates that large interference effects can exist between wing and body at transonic speeds.

The present paper reports the results for a configuration differing from that of reference 2 only in that the wing was located aft of the body maximum diameter. The results are presented as curves showing the variation of drag coefficients with Mach number for the complete configuration and for each of its component parts. Corresponding variations of drag coefficients are included from the results of reference 2 (wing mounted forward) for purposes of comparison.

## APPARATUS AND METHOD

Test configuration.- The general arrangement of the configuration is shown in figure 1 and its details and dimensions are given in figure 2. This wing-body combination differed from that of reference 2 only in the relative location of wing and body. (See fig. 2.) The  $45^\circ$  sweptback wing had a 70-inch span with NACA 65-009 sections and had a 12-inch chord perpendicular to the leading edge. The body had a fineness ratio of 12 and a maximum diameter of 10 inches at its midpoint. The 50-percent-root-chord station of the wing was located 15 inches aft of the maximum body diameter as compared to the 15-inch forward mounting tested previously. The wing entered the body through rectangular slots and was attached to a force-measuring balance inside the body. These slots were filled with wooden blocks which were faired to the body contour and attached to the wing at the root. A small clearance was allowed between the blocks and the sides of the slots so that the wing was free to move under the restraint of the balance.

Measurements.- Measurement of the desired quantities was accomplished as in previous tests (references 1 to 5) through use of the NACA radio telemetering system and radar and phototheodolite equipment. The following quantities were recorded at ground stations by the telemetering system:

- (1) The force exerted by the wing on the body as measured by a spring balance
- (2) The force exerted by the tail fins on the tail boom as measured by a spring balance
- (3) The retardation of the configuration as measured by a sensitive accelerometer aligned with the longitudinal axis of the body
- (4) The total pressure at an orifice located at the nose of the body as measured by an aneroid cell

The radar and phototheodolite equipment was used to record the path of the model during its fall. A survey of atmospheric conditions at the time of the test was obtained from synchronized records of static pressure, temperature, and geometric altitude during the descent of the airplane from which the configuration was dropped. The direction and velocity of the horizontal component of the wind was determined from radar and phototheodolite tracking records of the ascent of a free balloon immediately after the test.

Reduction of data.- The velocity variation of the model with respect to the ground, hereafter referred to as ground velocity, was obtained both by differentiation of the flight path as recorded by the radar and phototheodolite equipment and by a step-by-step integration of the vector sums of gravitational acceleration and the directed retardation as measured by the accelerometer. True airspeed was obtained by vector summation of ground velocity and horizontal wind velocity at appropriate altitudes.

The total drag was obtained by multiplying the retardation  $a_z$  (in g units) by the total weight. The drag force on the wing  $D_w$  was determined through use of the relation

$$D_w = R_w + W_w a_z$$

where

$R_W$  measured reaction between body and wing, pounds

$W_W$  weight of movable wing assembly, pounds

The drag of the tail fins was obtained from the same relation by using the reaction between the fins and the tail boom and the weight of the movable fin assembly. The body drag was determined by subtracting the drags of the wing and tail from the total.

Values of drag  $D$ , static pressure  $p$ , and frontal area  $F$  were combined to form the nondimensional parameter  $D/Fp$  for the complete configuration and each of its components. The Mach number  $M$  was determined from the absolute temperature  $T$  and the true airspeed. Values of the conventional drag coefficient based on frontal area  $C_{D_F}$  were obtained by use of the relation

$$C_{D_F} = \frac{D/Fp}{M^2 \gamma / 2}$$

where the ratio of specific heats  $\gamma$  was taken as 1.4. In the case of the wing and the tail fins, drag coefficients based on the plan area  $C_D$  were obtained by multiplying  $C_{D_F}$  by the ratio of frontal area to plan area. The areas used do not include that submerged in the body or the tail boom.

## RESULTS AND DISCUSSION

A time history of measured and computed quantities obtained from this test is given in figure 3. The variation of ground velocity shown as a dashed line on this figure was computed from the accelerometer data while the test points were computed from the radar and phototheodolite data. The scatter in the radar and phototheodolite data is larger than has been obtained in previous tests. This scatter results from a partial failure of some of the equipment during the test, which necessitated use of less precise auxiliary recording devices. These data show, however, that the velocity curve obtained from the accelerometer data closely fits the radar test points, which confirms the accuracy of the total-drag measurement.

The two Mach number variations shown in figure 3 were also obtained from two independent sets of measurements. The solid curve, which was computed from the ground velocity corrected for wind (airspeed) and the temperature data, is believed accurate to within  $\pm 0.01$  in Mach number. All results presented herein are correlated on the basis of this Mach number. The dashed curve was obtained from the telemetered records of total pressure and from the static pressure as determined from the geometric height of the body and the atmospheric survey. The two Mach number curves show good agreement except during the last 10 seconds of the fall where the difference in the Mach numbers is larger than the estimated error in the Mach number computed from the pressure measurement. The data presented have been corrected for the total-pressure loss through the normal shock, but this correction is small relative to the magnitude of the discrepancy. This condition where total pressure measurements give too low a Mach number during the later part of the fall (low altitude - high Mach number) has occurred for other tests (see reference 3) and will be investigated further.

The results of this test are presented in figures 4 to 8 as curves showing the variations with Mach number of the parameter  $D/F_p$  and drag coefficients for the complete configuration and each component. Corresponding curves are also presented for the wing-body combination whose test was reported in reference 2 (wing mounted forward). For both tests the drag forces were measured to within  $\pm 7$  pounds for the complete configuration,  $\pm 3\frac{1}{2}$  pounds for the wing, and  $\pm 1\frac{1}{2}$  pounds for the tail. The accuracy with which the drag parameters were determined varied throughout the fall due to the variation in static pressure, and in the case of the drag coefficients, the accuracy was also affected by the Mach number. The maximum estimated uncertainty of these drag parameters for several Mach numbers is presented in the following table:

Mach number	0.8			1.0			1.2		
	D/Fp	C <sub>D<sub>F</sub></sub>	C <sub>D</sub>	D/Fp	C <sub>D<sub>F</sub></sub>	C <sub>D</sub>	D/Fp	C <sub>D<sub>F</sub></sub>	C <sub>D</sub>
Total	0.011	0.028	-----	0.007	0.017	-----	0.003	0.007	-----
Wing	.012	.029	0.0018	.009	.016	0.0010	.004	.008	0.0005
Tail	.032	.073	.0044	.023	.044	.0026	.010	.019	.0011
Body	.034	.078	-----	.024	.033	-----	.010	.013	-----

As the body drag was not measured directly, the error in the body drag was taken as the sum of the errors for the other components. For

this reason the body drag parameters are probably more accurate than indicated by the table.

The variations with Mach number of  $D/F_p$  and drag coefficients based on total frontal area for the complete configuration are given in figure 4. The drag per unit frontal area rose from 0.045 of atmospheric pressure at a Mach number of 0.93 to 0.126 of atmospheric pressure at  $M = 1.03$  and then increased almost linearly to 0.233 at  $M = 1.24$ . The cross hatching on figure 4 shows how the total drag was divided among its components. The wing produced about one-half of the total drag at Mach numbers in excess of unity and the body produced about one-third the drag in the same Mach number range. The remaining drag was contributed by the tail fins.

Comparison of the total drag for the wing-body combinations with the wing aft and with the wing forward is given in figure 5 as variations of  $D/F_p$  and  $C_{D_F}$  with Mach number. The drag with the wing aft was appreciably lower than the drag with the wing forward. Further, the abrupt drag rise occurred at about 0.05 lower Mach number for the wing-forward configuration. The total drag of the wing-aft configuration was about 35 percent lower than that of the wing-forward configuration at Mach numbers near 1.00, and this difference decreased to about 10 percent at  $M = 1.18$ . These differences in total drag resulting solely from the change in the position of the wing on the body definitely establish the presence of large interference effects between wing and body.

The variations of  $D/F_p$ ,  $C_{D_F}$ , and  $C_D$  for the wing of the present configuration are given in figure 6. The drag per unit frontal area of this wing rose abruptly from 0.037 of atmospheric pressure at a Mach number of 0.95 to 0.137 of atmospheric pressure at  $M = 1.03$  and then increased linearly to 0.289 at  $M = 1.24$ . The drag of the wing in the forward position, reproduced in figure 6 from reference 2, shows a similar abrupt rise near  $M = 1$ . This abrupt rise in drag was absent in the results of tests of sweptback airfoils mounted on cylindrical bodies reported in reference 4. These combined results indicated that, at transonic speeds, the drag of a swept wing is apparently dependent upon the shape of the body on which it is mounted.

Comparison of wing drags for the two positions of the wing on the body shows that the drag was slightly higher through the Mach number range investigated when the wing was mounted in the forward position. Further, the abrupt rise in wing drag with the wing mounted forward took place approximately 0.03 lower in Mach number. This difference in the wing drags may possibly result from buoyancy effects due to the presence of the body. With the wing mounted in the forward

position, the pressure gradient caused by the body in the vicinity of the wing root probably tends toward increasingly negative pressures from leading to trailing edge. A smaller or opposite gradient probably exists for the case of the wing in the aft position. The phenomenon which produces the earlier drag rise when the wing is in the forward position is not understood, for if the expected pressure distribution exists over the body, the root of the wing located in the aft position would be in a region of higher local velocities than the root of the wing located in the forward position. The case where the wing root is in a region of higher local velocities (wing aft) would normally be considered the more critical from the standpoint of the drag rise.

The variations of the tail-drag parameters with Mach number are presented in figure 7. For the present test, the drag per unit frontal area of the tail fins rose abruptly from 0.028 of atmospheric pressure at a Mach number of 0.875 to 0.331 of atmospheric pressure at  $M = 1.0$  and then increased at a slower rate to 0.49 at  $M = 1.24$ . Drag curves are also presented in figure 7 from tests of two other sets of identical tail fins. One set was tested on the wing-forward configuration (reference 2) and the other was tested on a body of fineness ratio 6 without wings (reference 5). Generally, the three drag curves are in good agreement. However, the differences that exist are larger than would be expected from the uncertainties in the measuring system.

The variations with Mach number of  $D/F_p$  and  $C_{D_F}$  for the body of the present configuration are shown in figure 8. The drag per unit frontal area increased slowly to 0.053 of atmospheric pressure at  $M = 0.93$  and then decreased slightly to 0.042 at  $M = 0.96$ . Further increase in Mach number resulted in a steady increase in  $D/F_p$  to 0.09 at a Mach number of 1.03 and then to 0.15 at  $M = 1.24$ . Comparable data presented in figure 8 for the body of the wing forward configuration also show a slight decrease in  $D/F_p$  near  $M = 0.96$ . The actual existence of this small drag decrease has not been definitely determined, however, since this variation is well within the accuracy of the drag measurement.

The measured drag variation with Mach number for the body tested without wings (reference 1) is shown in figure 8. The body without wings had the same stabilizing tail-fin arrangement as the other two configurations, but the drag of these fins was not measured separately. To obtain the drag of this body without fins an average value of tail drag, as obtained from the variations shown in figure 7, was subtracted from the drag of the body plus tail. In the range of Mach numbers for which drag variations for the body alone are presented on figure 8, the tail drag is small in comparison to the body drag and the small differences in the tail-drag variations shown in figure 7 have little effect on drag of the body alone.

At Mach numbers in excess of unity the body drag obtained from the present test (wing aft) was appreciably less than the basic body drag. (See fig. 8.) The body drag obtained from reference 2 (wing forward) was slightly higher than the basic body drag. With the wing in the forward position, the body drag was about 70 percent higher than the body drag with the wing in the aft position at Mach numbers near 1.03, and this difference decreased to 24 percent higher at  $M = 1.19$ . These differences in body drag account for the major part of the difference in the total drag of the two configurations. These results indicate that, for this type of wing-body combination, large interference effects exist on the body due to the presence of the wing and that these interference effects show a large variation between the two tested wing positions. The nature of these interference effects is not known at present, but possibly the presence of the sweptback wing in the aft location delays separation of the flow about the body.

#### CONCLUDING REMARKS

The drag of a wing-body combination has been measured at transonic velocities by the free-fall method. This configuration consisted of a  $45^\circ$  sweptback wing mounted behind the maximum diameter of the body of a body-tail arrangement whose drag characteristics without wings are known from a previous test.

The results show that the drag per unit frontal area for the complete configuration rose from 0.045 of atmospheric pressure at a Mach number of 0.93 to 0.126 at a Mach number of 1.03 and then increased almost linearly to 0.233 at a Mach number of 1.24. At Mach numbers above 1.0 the wing produced one-half of the total drag and the body produced about one-third. The remaining drag was contributed by the stabilizing tail surfaces.

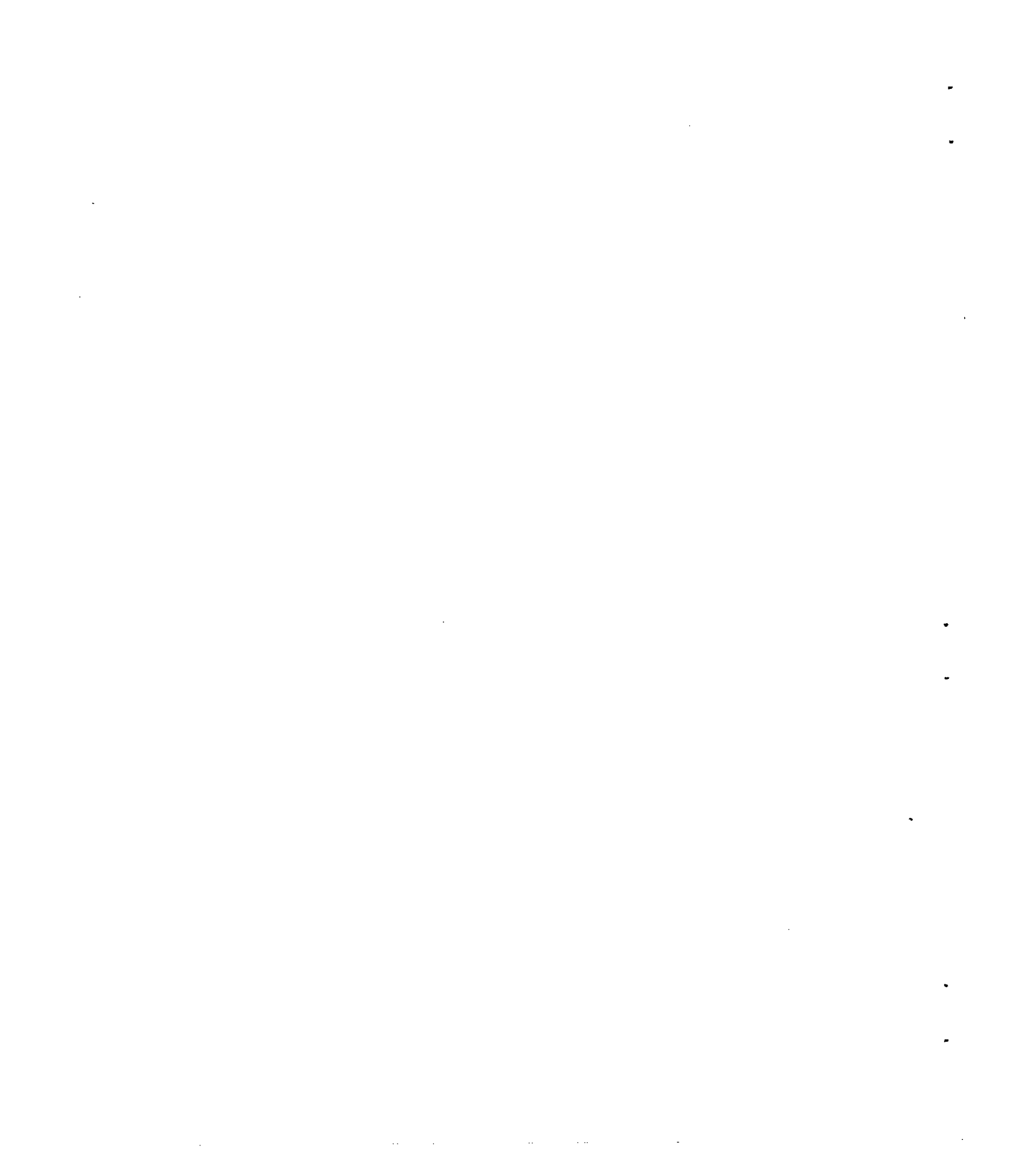
Comparison of these results with previous results for a configuration differing only in the location of the wing (forward of the maximum diameter) shows that the wing-aft configuration had 35-percent lower drag at a Mach number of 1.03 and 10-percent lower drag at a Mach number of 1.18. Most of this drag difference resulted from differences in the body drag of the two configurations. With the wing forward, the body drag was slightly higher than the drag of the body without wings, while with the wing aft, the body drag was appreciably lower than the drag of the body without wings. Thus, for this type of wing-body configuration large interference effects of the wing on the body exist and these interference effects show large variations between the two tested wing positions.

The wing drag for both configurations showed an abrupt rise near a Mach number of 1 which did not occur in previous tests of sweptback airfoils mounted on cylindrical bodies. This rise evidently is an interference effect caused by the presence of the body and appears to depend on the shape of the body. The rise, however, is small in comparison to the drag rise associated with rectangular airfoils.

Langley Memorial Aeronautical Laboratory  
National Advisory Committee for Aeronautics  
Langley Field, Va.

#### REFERENCES

1. Thompson, Jim Rogers, and Mathews, Charles W.: Total Drag of a Body of Fineness Ratio 12 and Its Stabilizing Tail Surfaces Measured during Free Fall at Transonic Speeds. NACA CB No. L6D08, 1946.
2. Mathews, Charles W., and Thompson, Jim Rogers: Free-Fall Measurements at Transonic Velocities of the Drag of a Wing-Body Configuration Consisting of a  $45^\circ$  Swept-Back Wing Mounted Forward of the Maximum Diameter on a Body of Fineness Ratio 12. NACA RM No. L6L26, 1947.
3. Mathews, C. W., and Thompson, J. R.: Measurements of Static and Total Pressure Throughout the Transonic Speed Range as Obtained from an Airspeed Head Mounted on a Freely Falling Body. NACA RM No. L7C04a, 1947.
4. Mathews, Charles W., and Thompson, Jim Rogers: Drag Measurements at Transonic Speeds of NACA 65-009 Airfoils Mounted on a Freely Falling Body to Determine the Effects of Sweepback and Aspect Ratio. NACA RM No. L6K08c, 1947.
5. Bailey, F. J., Jr., Mathews, Charles W., and Thompson, Jim Rogers: Drag Measurements at Transonic Speeds on a Freely Falling Body. NACA ACR No. L5E03, 1945.



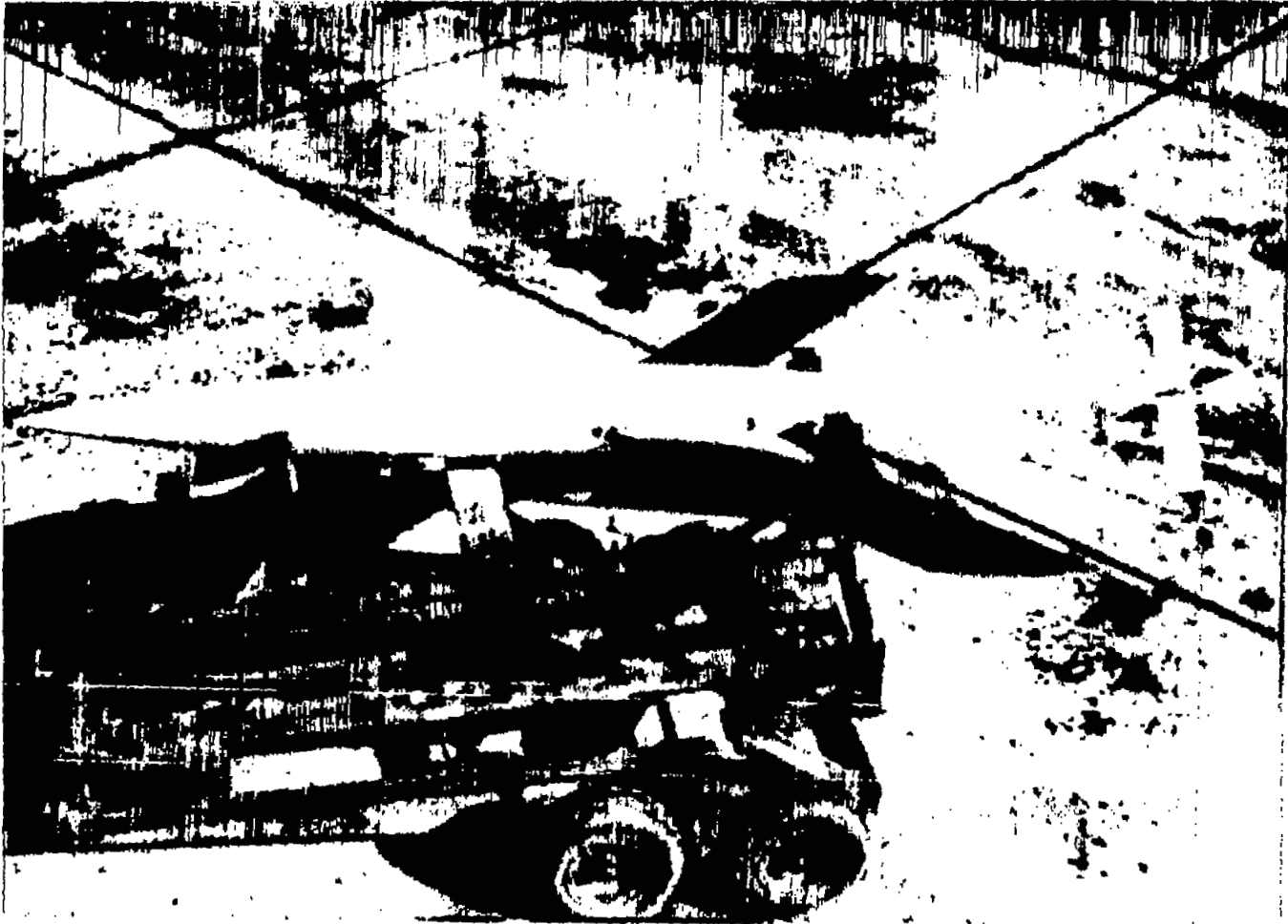
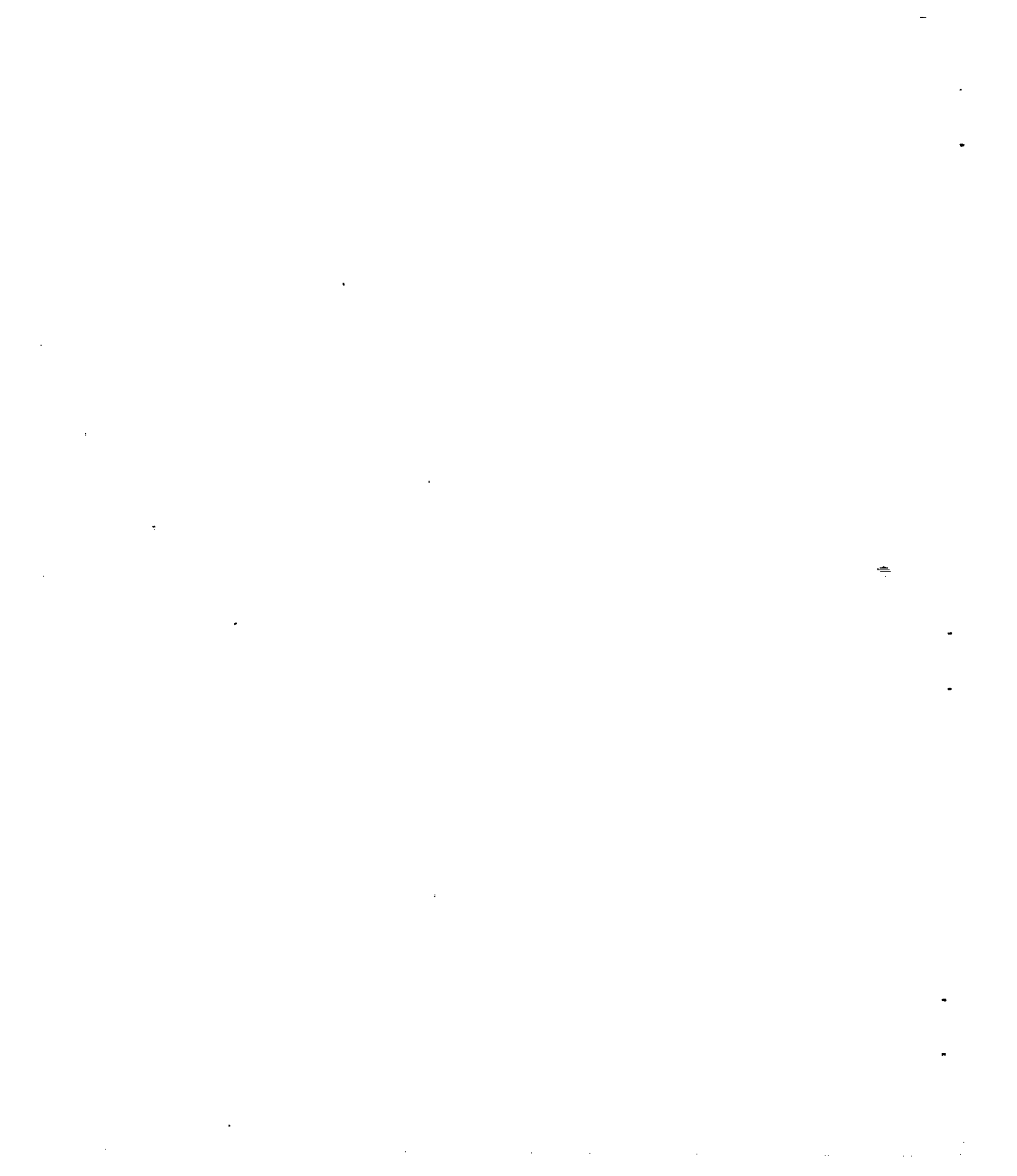
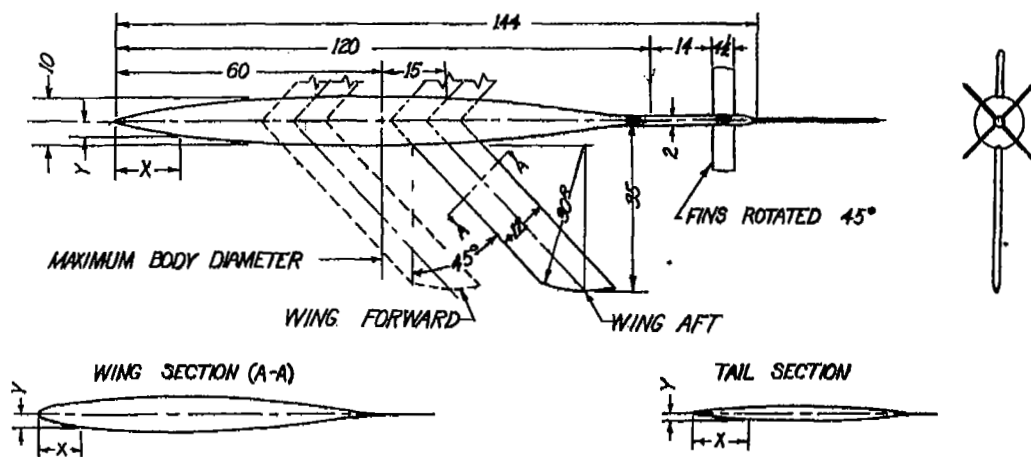


Figure 1.- General view of wing-body configuration with wing mounted aft of body maximum diameter.





AREAS, SQ FT	
BODY FRONTAL AREA	0.545
WING FRONTAL AREA	.438
TAIL FRONTAL AREA	.074
WING PLAN AREA	6.99
TAIL PLAN AREA	1.232
TOTAL FRONTAL AREA	1.057

BODY COORDINATES			
X	Y	X	Y
00	0.000	480	4.876
6	.277	540	4.971
9	.358	600	5.000
15	.514	660	4.955
30	.866	720	4.828
60	1.446	780	4.610
90	1.936	840	4.274
120	2.365	900	3.754
180	3.112	960	3.031
240	3.708	1020	2.222
300	4.159	1080	1.350
360	4.489	1140	.526
420	4.719	1200	.000
NOSE RADIUS		0.060	

WING-SECTION COORDINATES (NACA 65-009 SECTION)					
X	Y	X	Y	X	Y
0.00	0.000	2.40	0.447	7.80	0.398
.06	.083	3.00	.486	8.40	.342
.09	.102	3.60	.512	9.00	.280
.15	.127	4.20	.531	9.60	.216
.30	.171	4.80	.540	10.20	.151
.60	.235	5.40	.537	10.80	.088
.90	.286	6.00	.520	11.40	.033
1.20	.328	6.60	.490	12.00	.000
1.80	.396	7.20	.448		
L.E. RADIUS		0.066			

TAIL-SECTION COORDINATES (NACA 16-0018 SECTION)			
X	Y	X	Y
0.000	0.000	1.350	0.122
.052	.029	1.800	.132
.113	.041	2.250	.135
.225	.056	2.700	.131
.338	.068	3.150	.118
.450	.078	3.600	.094
.675	.093	4.050	.057
.900	.105	4.275	.032
1.125	.115	4.500	.008
L.E. RADIUS		0.008	

NATIONAL ADVISORY  
COMMITTEE FOR AERONAUTICS

Figure 2.- General arrangement and dimensions of wing-body configuration with wing mounted aft of body maximum diameter. All dimensions are in inches. Wing sections measured perpendicular to leading edge.

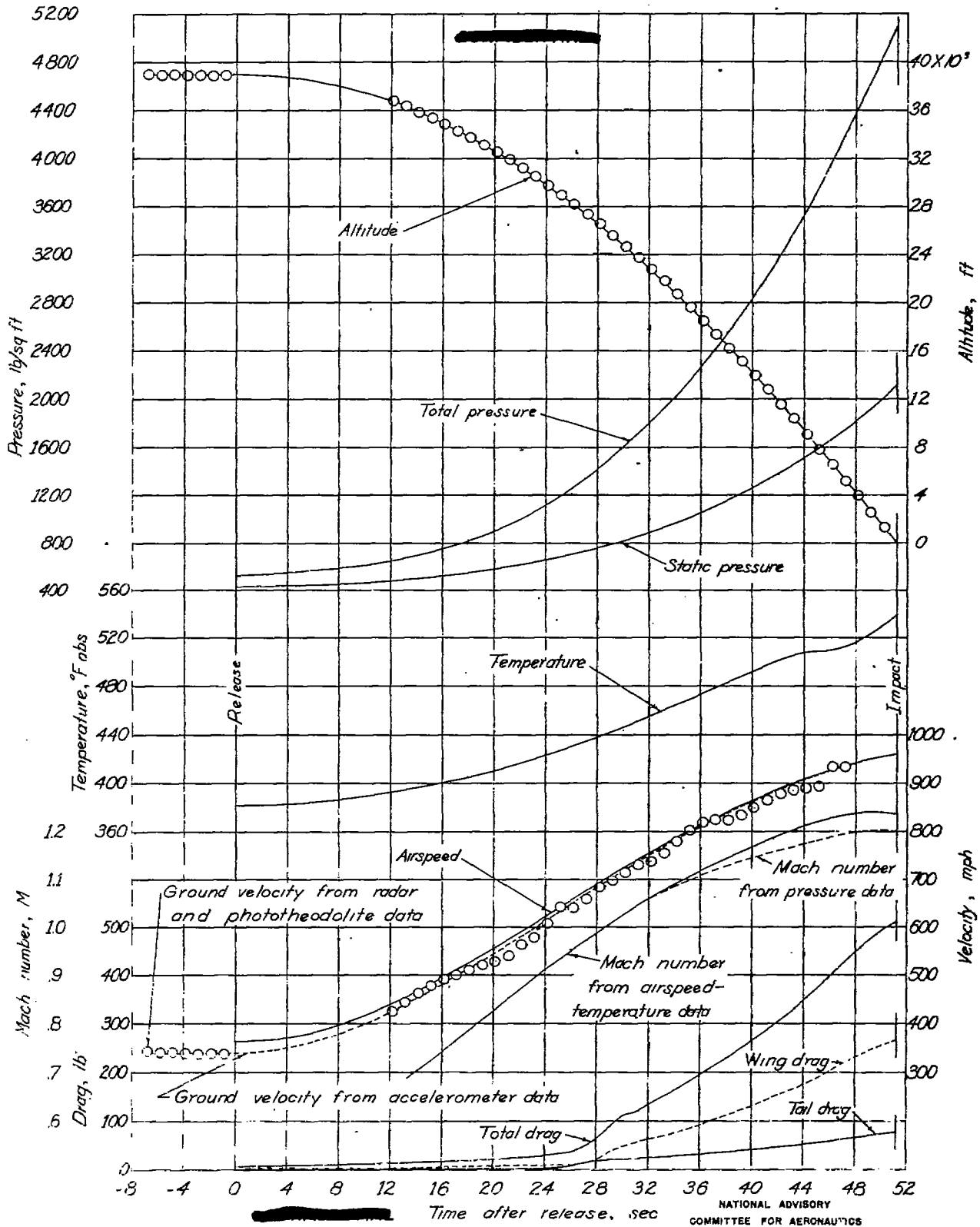


Figure 3.- Time history of free fall of wing-body configuration with wing mounted aft of body maximum diameter.

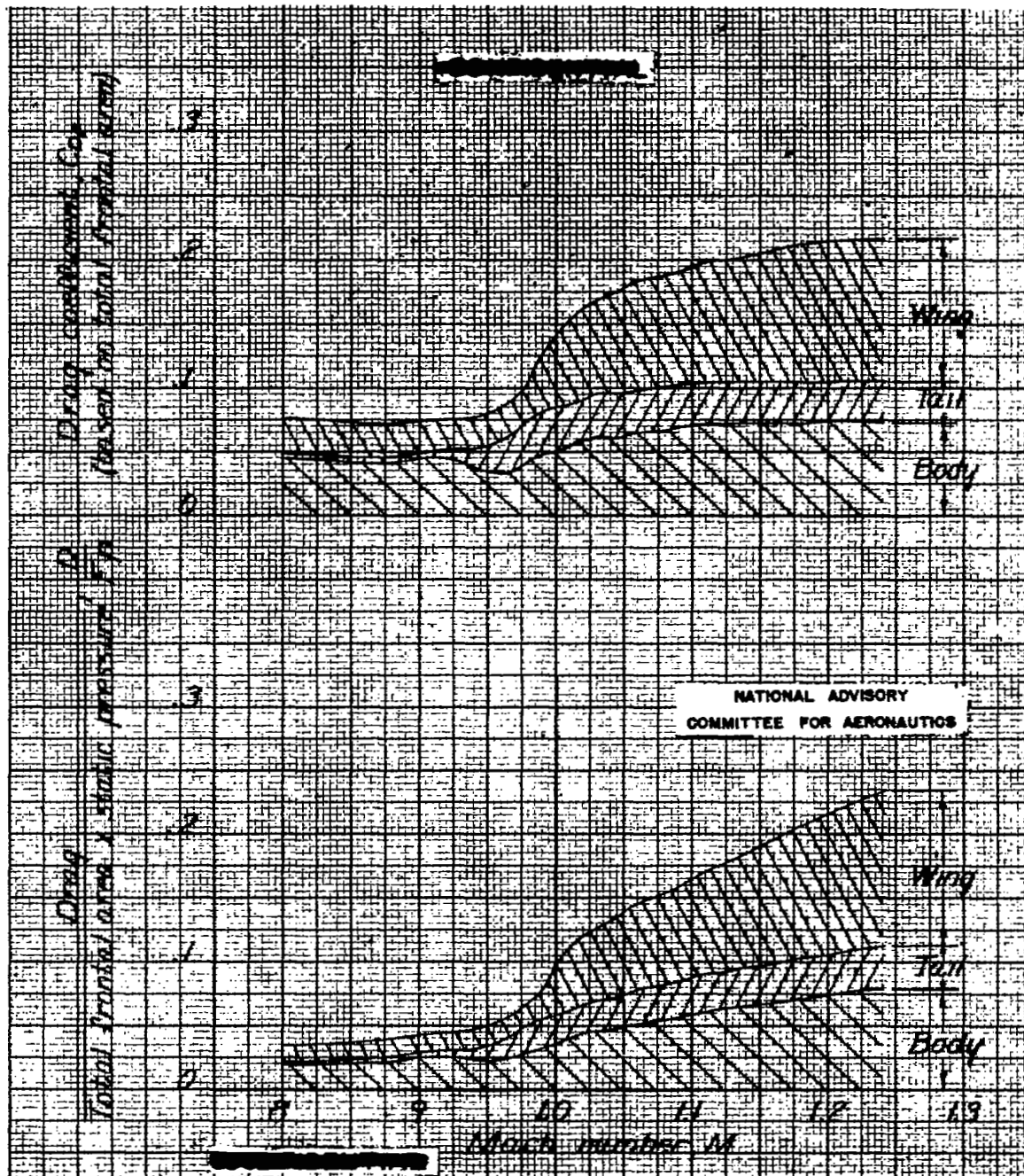


Figure 4.- Variation with Mach number of drag coefficient and  $D/F_p$  for the wing-body configuration with wing mounted aft of body maximum diameter.

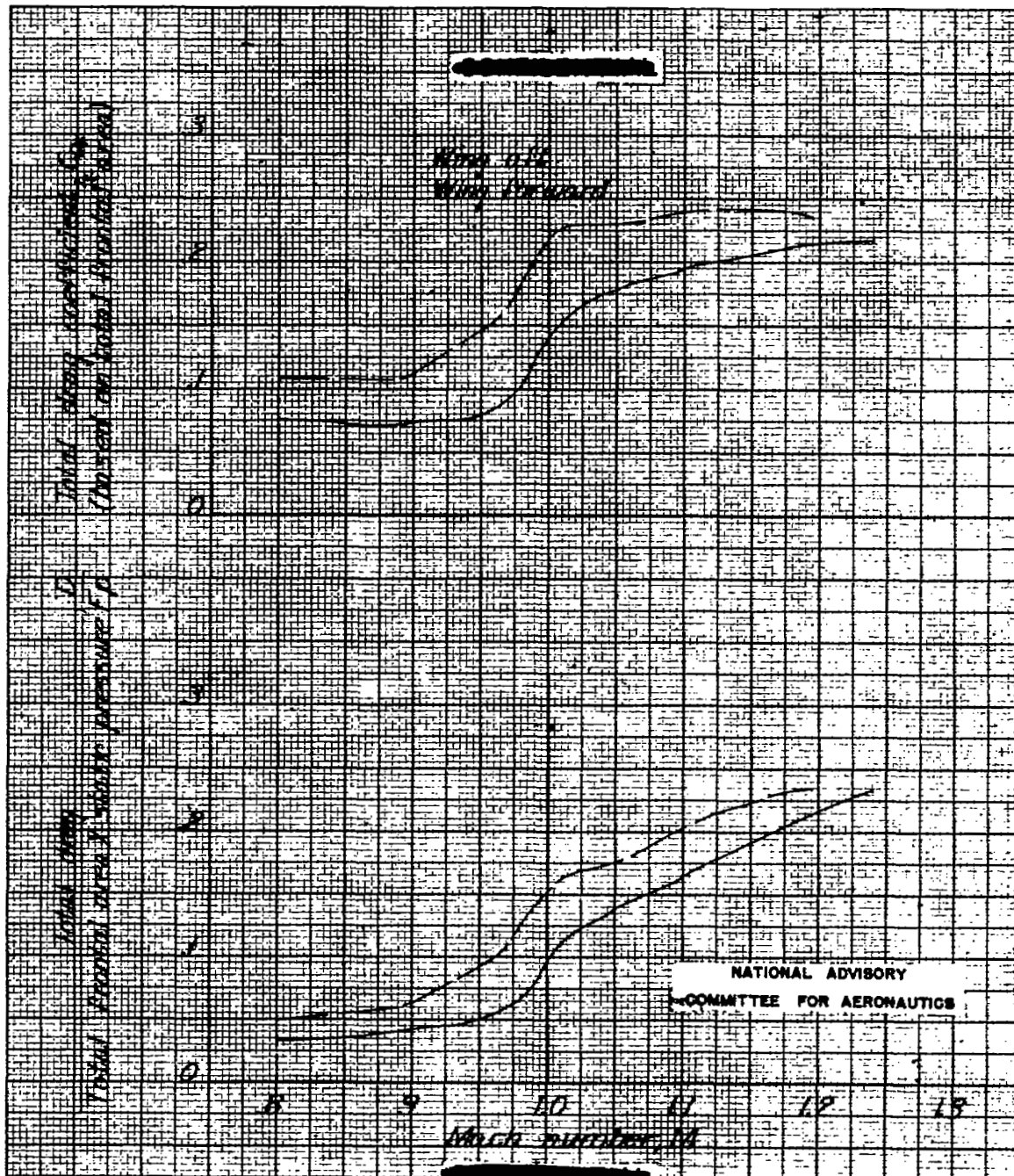


Figure 5.- Comparative variations with Mach number of drag coefficient and  $D/F_p$  for the wing-aft configuration and the wing-forward configuration.

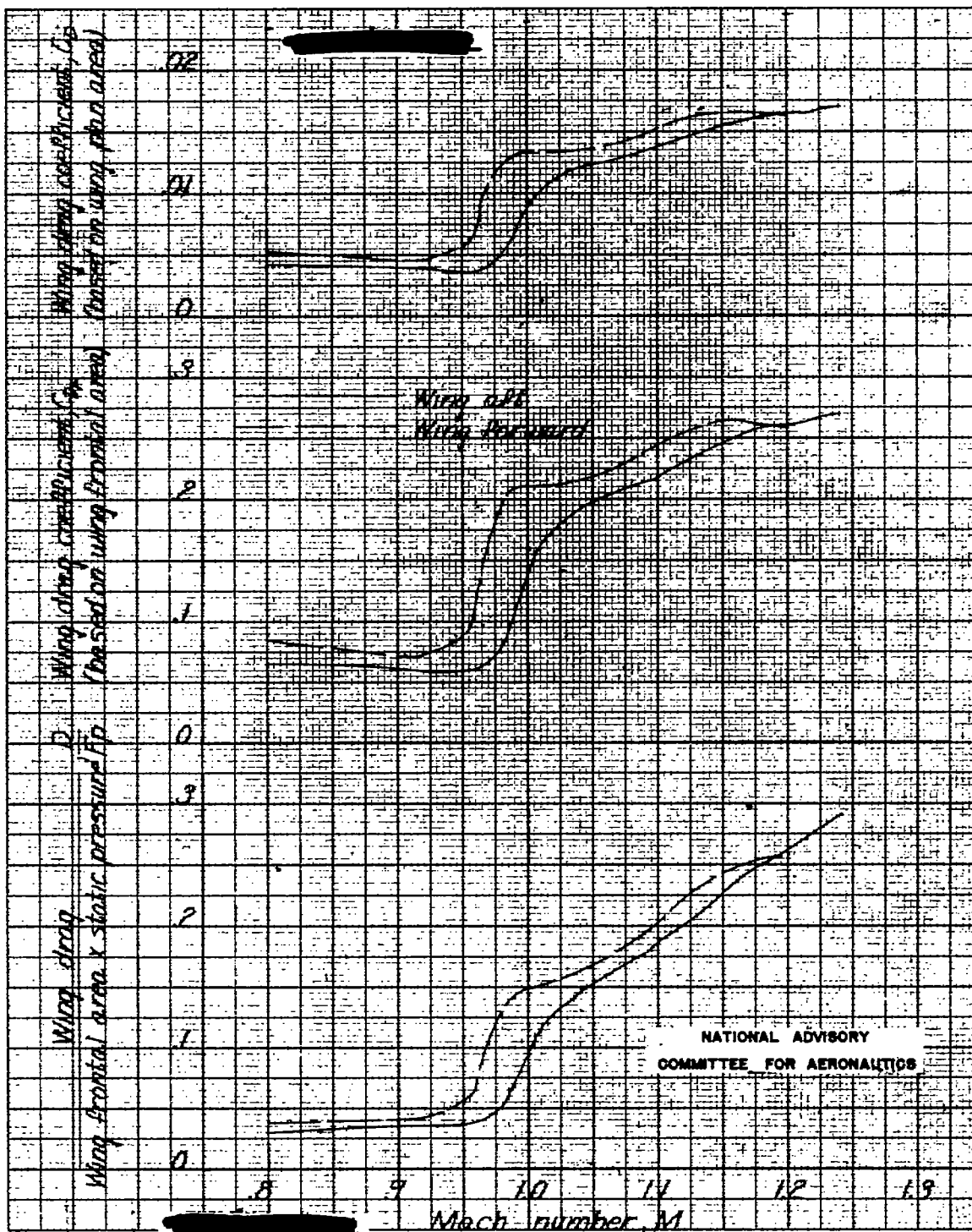


Figure 6.- Comparative variations with Mach number of drag coefficients and  $D/F_p$  for the  $45^\circ$  sweptback wing of the wing-aft configuration and the wing-forward configuration.

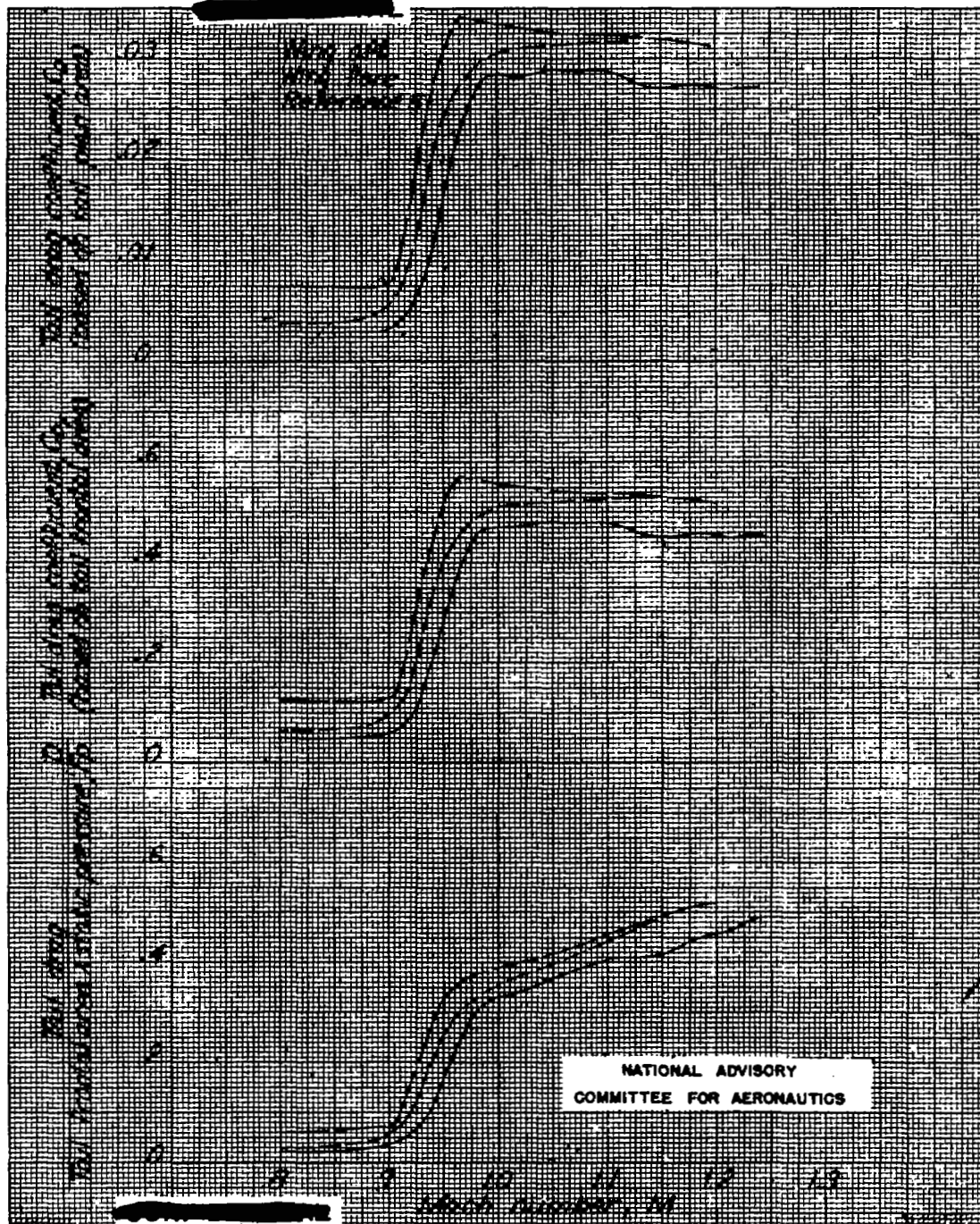


Figure 7.- Comparative variations with Mach number of drag coefficients and  $D/F_p$  for the tail fins of the wing-aft configuration and the wing-forward configuration. Data also presented for identical tail fins mounted on a body of fineness ratio 6 without wings.

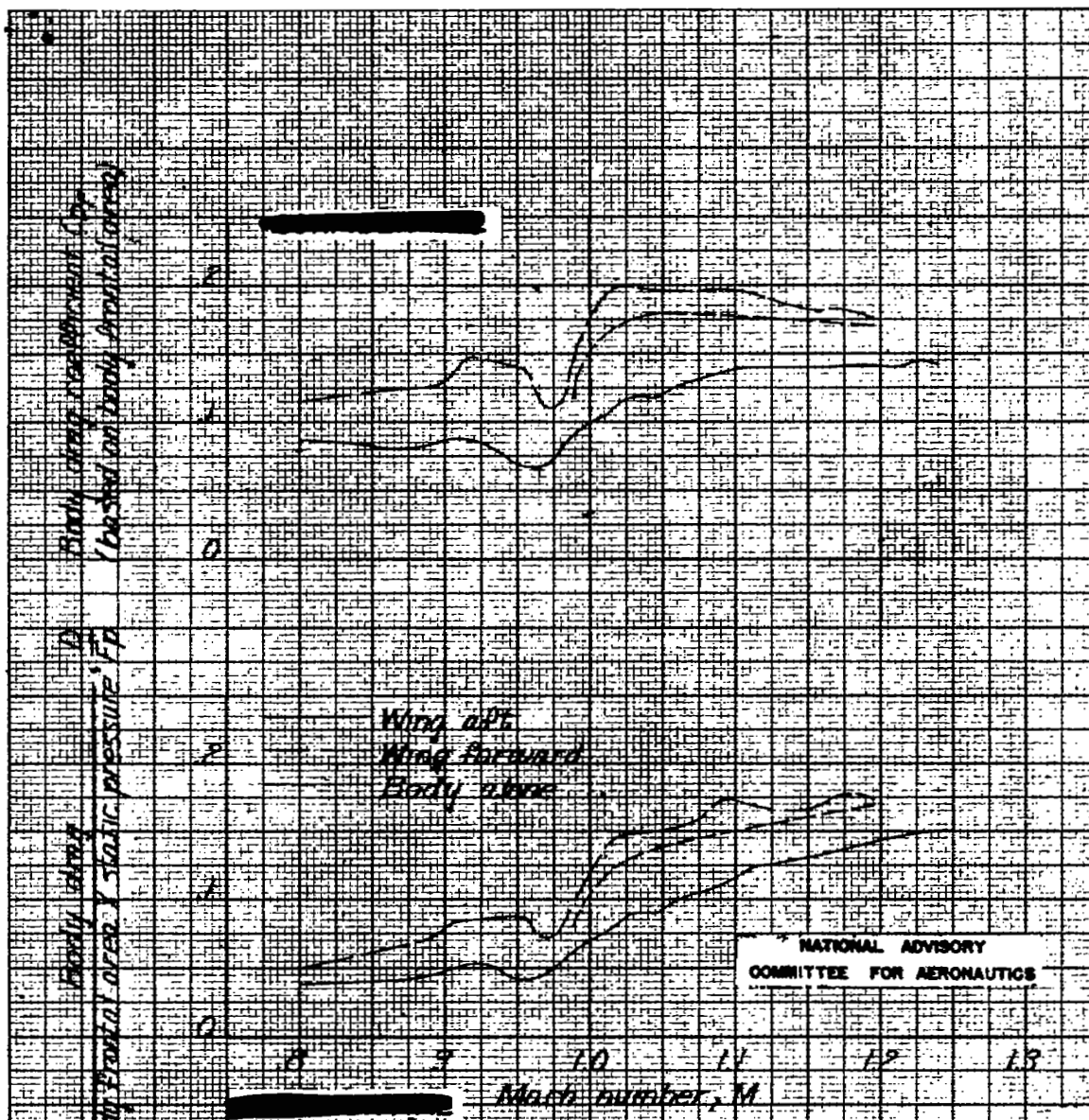


Figure 8.- Comparative variations with Mach number of drag coefficient and  $D/F_p$  for body of the wing-aft configuration and wing-forward configuration. Data also presented for identical body without wings.



**DO NOT REMOVE SLIP FROM MATERIAL**

Delete your name from this slip when returning material to the library.

NAME	DATE	MS
<del>David Meiri</del>	<del>11/3/97</del>	<del>153</del>

NASA Langley (Rev. Dec. 1991)

RIAD N-75